CHAPTER 5

LABORATORY ANALYSES

Introduction

To understand the depositional dynamics of any sedimentary system it is necessary to understand not only the sediment body geometries and physical structures in the field (as described in earlier chapter), but also to have detailed examination of its textural and compositional attributes. This shed light on the sediment source, pathways and burial at the place of the study. In this chapter the author has investigated the prime constituent under study- the miliolites for its grain size and related parameters as well as its constituents such as allochems, detritals, cement and ultra-structures and micro-chemistry using SEM-EDS. An attempt is also made to present primary data on its bulk magnetic susceptibility, of course with limited application. To understand the detrital interference and diagenesis of these rocks, limited samples were analyzed using XRF facility of the Institute of Seismological Research (ISR), Gandhinagar.

Textural Analysis

Textural characteristics of the miliolite samples were studied using conventional mechanical sieving technique for friable samples, whereas the indurated samples were subjected to thin section study. Granulometric analysis and statistical parameters for the friable miliolite samples were calculated following Folk and Ward (1957). 20 samples from the study area, including all three types of deposits, were subjected to the mechanical sieving procedure at half-phi interval. After coning and quartering about 50 gm of sample was poured in the sieve stake with ASTM 25, 35, 45, 60, 120, 170 and 230 sieves and kept on Endecotts sieve shaker,Octago 200 make sieve shaker for a run of 15 minutes. The weight retained in each sieve was measured using Mettler Toledo (Switzerland) make digital weighing scale and the data were analyzed using Gradistate software to calculate statistical parameters viz., Mean (Mz), Sorting (σc), Skewness (S_kØ) and Kurtosis (Kσ). The data thus obtained are presented in Table 5.1 and 5.2. The triangular plots were used to characterize the average nature of the samples (Fig. 5.1).

Aperture (Phi)	Class Weight Retained (gm) in Different Samples									
	(1)	(2)	(3)	(4)	(5)	(6)	(7)	(8)	(9)	(10)
Sample	GR47	GR50	GR51	GR52	GR53	GR54	GR54A	GR55	GR56	GR56A
Type Identity:	I	II	II	II	III	III	III	III	III	III
Analyst:	Rashmikant N Talati									
Date:	19/12/2017									
Initial Sample Weight (gm)	48.97	48.47	48.70	47.70	48.23	49.13	45.43	47.60	48.10	49.15
0.5	12.95	11.01	9.16	23.33	13.37	16.22	8.97	7.07	12.27	9.74
1.0	5.87	3.80	3.16	6.48	3.98	6.44	5.58	5.55	5.81	4.86
1.5	11.26	3.35	2.63	5.25	7.66	4.88	7.66	8.79	5.79	5.71
2.0	7.07	7.07	7.28	4.49	10.33	4.94	10.33	9.74	9.19	7.59
2.5	3.58	5.36	6.28	2.47	2.60	3.44	2.60	6.77	4.70	5.59
3.0	4.00	9.45	10.73	2.42	5.92	4.82	5.92	5.91	5.05	8.02
3.5	1.59	3.36	4.29	1.13	1.54	2.47	1.54	1.60	1.84	3.39
4.0	1.10	2.98	3.65	1.01	1.16	2.52	1.16	1.08	1.48	2.65
0	1.55	2.09	1.52	1.12	1.67	3.40	1.67	1.09	1.97	1.60
Mean (M_Z)	1.358	1.791	1.922	0.932	1.475	1.511	1.554	1.607	1.521	1.721
Sorting (σc)	1.084	1.266	1.256	0.987	1.145	1.477	1.130	1.020	1.177	1.207
Skewness (S_KØ)	0.241	-0.052	-0.174	0.661	0.146	0.444	0.135	0.044	0.134	0.019
Kurtosis (Kσ)	0.948	0.728	0.808	1.028	0.858	0.936	0.940	0.961	0.842	0.783
Mean (M_Z)	Medium Sand	Medium Sand	Medium Sand	Coarse Sand	Medium Sand	Medium Sand	Medium Sand	Medium Sand	Medium Sand	Medium Sand
Sorting (σc)	Poorly Sorted	Poorly Sorted	Poorly Sorted	Moderately Sorted	Poorly Sorted	Poorly Sorted	Poorly Sorted	Poorly Sorted	Poorly Sorted	Poorly Sorted
Skewness (S_KØ)	Fine Skewed	Symmetrical	Coarse Skewed	Very Fine Skewed	Fine Skewed	Very Fine Skewed	Fine Skewed	Symmetrical	Fine Skewed	Symmetrical
Kurtosis (Kσ)	Mesokurtic	Platykurtic	Platykurtic	Mesokurtic	Platykurtic	Mesokurtic	Mesokurtic	Mesokurtic	Platykurtic	Platykurtic

Table-5.1. Results of the granulometric analysis of the samples from Gangeswar Area (GA).

Aperture (Phi)	Class Weight Retained (gm) in Different Samples									
	(1)	(2)	(3)	(4)	(5)	(6)	(7)	(8)	(9)	(10)
Sample	FR28	FR29A	FR29	FR30	FR31	FR32	FR33	FR41	FR42	FR45
Type Identity:	III	III	III	I	II	I	I	II	II	III
Analyst:	Rashmikant N Talati									
Date:	20/12/2017									
Initial Sample Weight (gm)	48.97	48.47	48.70	47.70	48.23	49.13	45.43	47.60	48.10	49.15
0.5	17.64	10.74	9.45	25.41	9.45	16.00	24.47	3.01	10.57	9.94
1.0	5.29	4.92	4.96	4.42	4.96	5.95	5.31	5.07	5.34	4.08
1.5	3.93	3.92	4.18	3.62	4.18	4.59	4.10	4.45	2.78	3.40
2.0	4.40	3.43	3.50	3.31	3.50	4.44	3.30	7.63	8.06	8.33
2.5	2.28	2.66	2.41	2.22	2.41	3.26	1.68	5.02	3.79	6.31
3.0	3.50	3.31	4.64	2.57	4.64	6.24	2.36	9.59	5.43	8.71
3.5	2.93	3.29	3.19	1.79	3.19	3.56	1.80	6.37	4.59	4.21
4.0	4.27	6.02	7.26	2.50	7.26	3.19	2.04	4.27	3.50	2.53
0	4.54	10.58	9.35	3.46	9.35	1.93	4.28	3.29	4.94	1.70
Mean (M_Z)	1.666	2.550	2.506	1.201	2.506	1.545	1.244	2.275	1.929	1.795
Sorting (σc)	1.719	2.224	2.091	1.476	2.091	1.296	1.579	1.323	1.692	1.230
Skewness (S_kØ)	0.521	0.287	0.170	0.800	0.170	0.322	0.796	-0.004	0.237	-0.063
Kurtosis (Kσ)	0.914	0.891	0.930	1.156	0.930	0.677	1.340	1.133	0.996	0.768
Mean (M_Z)	Medium Sand	Fine Sand	Fine Sand	Medium Sand	Fine Sand	Medium Sand	Medium Sand	Fine Sand	Medium Sand	Medium Sand
Sorting (σc)	Poorly Sorted	Very Poorly Sorted	Very Poorly Sorted	Poorly Sorted	Very Poorly Sorted	Poorly Sorted	Poorly Sorted	Poorly Sorted	Poorly Sorted	Poorly Sorted
Skewness (S_kØ)	Very Fine Skewed	Fine Skewed	Fine Skewed	Very Fine Skewed	Fine Skewed	Very Fine Skewed	Very Fine Skewed	Symmetrical	Fine Skewed	Symmetrical
Kurtosis (Kσ)	Mesokurtic	Platykurtic	Mesokurtic	Leptokurtic	Mesokurtic	Platykurtic	Leptokurtic	Leptokurtic	Mesokurtic	Platykurtic

Table 5.2 Results of the granulometric analysis of the samples from Fakirwadi area (FA).

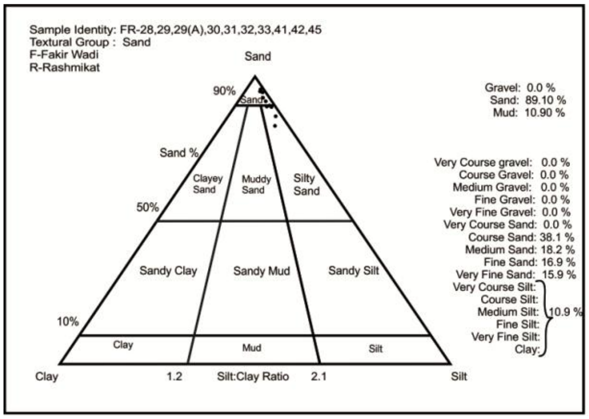

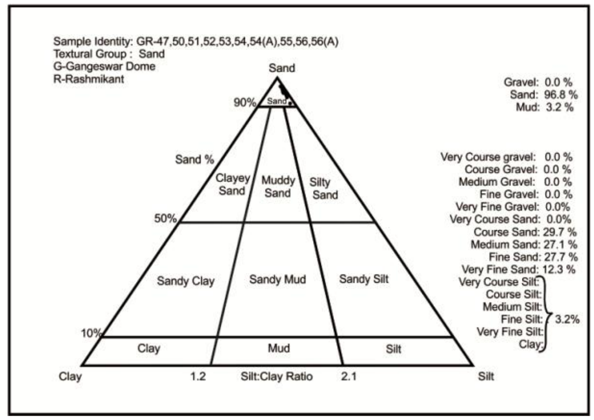

Fig.5.1 Grain size data of the friable miliolite samples plotted on triangular diagram using the Gradisat software.

The granulometric analysis suggests that majority of the grains are of sand size ranging from 0.9 phi to 2.5 phi, moderately to poorly sorted, finely skewed and having platykurtic to mesokurtic distribution. Table 5.3 presents an average nature of three types of deposits for its granulometric studies.The Type-I deposits have grain size range between 1.2 and 1.6 phi with an average grain size 1.4 phi, whereas Type II and Type-III grain size range from 0.9 to 2.5 phi with average grain size of 1.9 phi. Type-I Miliolite shows better sorting, whereas the Type-II and III poor. Type-I Miliolites exhibit very fine skewed and Type-II Miliolites exhibit mixed skewed nature, whereas Type-III shows fine to symmetrical skewed nature. Type-I shows Leptokurtic to Mesokurtic distribution, while Type II and III shows Mesokurtic to Platykurtic distribution. This suggest an increased influence of the locally derived sediments being mixed with the original aeolian sediments that occurs as the Type-I Miliolite deposits in the study area.

Type of deposit	Grain size range (M_Z)	Mean (M_Z)	Average grain size (phi)	Sorting (σc)	Skewness (S_kØ)	Kurtosis (Kσ)
Type-I N=04	1.2 to 1.6	Medium Sand	1.4	1.0 to 1.5	Very Fine Skewed	Leptokurtic to Mesokurtic
Type-II N=06	0.9 to 2.5	Fine to Medium	1.9	0.98 to 2.0	mixed	Mesokurtic to Platykurtic
Type-III N=10	1.4 to 2.5	Fine to Medium	1.9	1.1 to 2.2	fine to symmetrical	Mesokurtic to Platykurtic

Table 5.3 Summary of the granulometric study of three types of Miliolite deposits.

Kotda study area (KA) and Varli study area (VA) exhibits similar grain size characteristics under the microscope and as they are indurated in nature were not suitable for the mechanical sieving technique.

Compositional Analysis

Insoluble Residues

To evaluate the proportional amount of non carbonate acid insoluble residues and the carbonate content, variety of miliolitic deposits of indurated, friable and loose sand samples from the different location of the study area were analyzed. Total 10 gm weight of each sample was taken for dissolving in 10 N HCL for 24 hours. After washing with hot distilled water and filtering process remaining residues were put in oven at 50^{o}C for an additional 24 hours to remove moisture. The residues were weighed and proportional amount was calculated in terms of the weight loss percentage (Table 5.4). Also the residues were observed under binocular microscope that shows mainly the presence of quartz, rock fragments of sand stone and basalt, laterite, silt and clay.

Determination of the 'relative' or the 'absolute' amount of residues and the carbonate content provide important clues in understanding the process of accumulation and deposition of carbonate sands of Kachchh. The residue analysis has indicated that the miliolitic deposits, Type-I Miliolite contains about 41 % of residue by weight, whereas it is ca. 55% in Type-II and highest (ca. 70%) in Type-III Miliolites (Fig. 5.2).

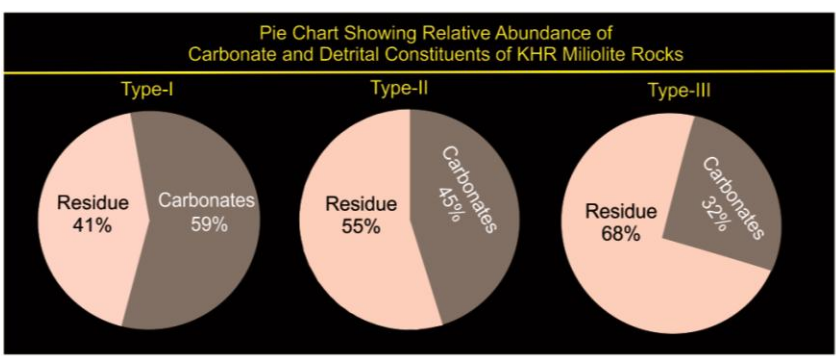

Fig. 5.2 Relative abundances of Carbonate and Residue constituent of Miliolite Rocks, KHR, Kachchh.

This terrigenous content is on account of the altitude of the site of deposition and type of the source rock available near the site of deposition of miliolitic sand.

Thin Section Study

For petrographic studies, thin sections were prepared and studied under microscope, following the procedure of Folk (1959). The first part of the rock name refers to the allochem components and the second part to the cementing or matrix material. The Folk's terminologies were adopted in the study of the thin sections of the Miliolite limestone. The volumetric analysis of different constituents had done with the help of average manual counter, for the petrographical classification of limestone.

All the thin sections were prepared in the thin section laboratory at Geology Department, the Maharaja Sayajirao University of Baroda. Initially the rock wafers slice were prepared by cutting of the rocks into small pieces using 'Struers' Geological Rock Cutter. One side of the rock wafers were grinded to make it smooth using rock sample after subjecting it to abrasion with water and 100 Mesh Aladum and 400 mesh Carbodudum grade polishing powder on Struers made Labopole-35 grinding and polishing. Then the smooth sides of the rock chips were mounted on glass slide using Araldite / Canada balsam. At the time of mounting, care was taken to make sure no air bubble is present within the glass slides.

Optical microscopy was done using these thin sections in transmitted light under the 'LEICA DM4 P, DM2700 P, DM750P' Polarizing Microscope. The digital images from an optical microscope were captured by constant color temperature LED light-technology sensitive cameras and images were saved in digital format with comprehensive Leica Application Suite (LAS) and connected computational software facility.

The 21 samples which were suitable for thin section making were studied for its textural and compositional characteristics under the petrological microscope. Thin sections study of miliolites to determine nature of the sediments three main components distinguished on the basis of average manual counter petrographic data are various allochems (bioclasts and peloids) and detrital (Fig. 5.3; Table 5.4). The allochemical contents are characterized by the dominance of peloids (10-40%) followed by the bioclasts (10-30%). The detrital grains are also contributing to a significant amount 35-80%. The acid insoluble residue analysis also supports the above result. Average among them the detrital found highest about 53% and above, peloids is in between 26% and bioclasts is lowest 21% existence determined (observed).

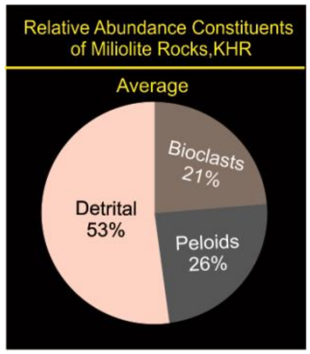

Fig. 5.3 Abundance constituents of Miliolites of the study area.

The bioclasts observed are foraminifers, echinoderm, brachiopods gastropods, bryozoans, algae,croal and shell fragments etc (Fig. 5.4). They are sand size medium grained, sub angular well rounded to sub rounded, well sorted and less compacted, showing point and long contact, allochthounous in nature, first generation microsparite and second generation sparite cement. Orthochemical component is cements and are calcareous. The cement is mostly microsparite (1^{st} order) and sparite (2^{nd} order), having law magnesian non-ferroan calcite composition and meniscus, rim or gravitational cement geometry and fibrous type also found, which were reported earlier by Patel and Allahabadi (1988).On the basis of relatively abundances and cement type and nature from the microscopic study of the samples the miliolite rocks of study area and are accordingly and have been broadly classified on the basis of studies following the Folks classification (Folk, 1959, 1962) as i.e. biopellsparite / pellbiosparite / oobiopellsparite (Fig.5.4).

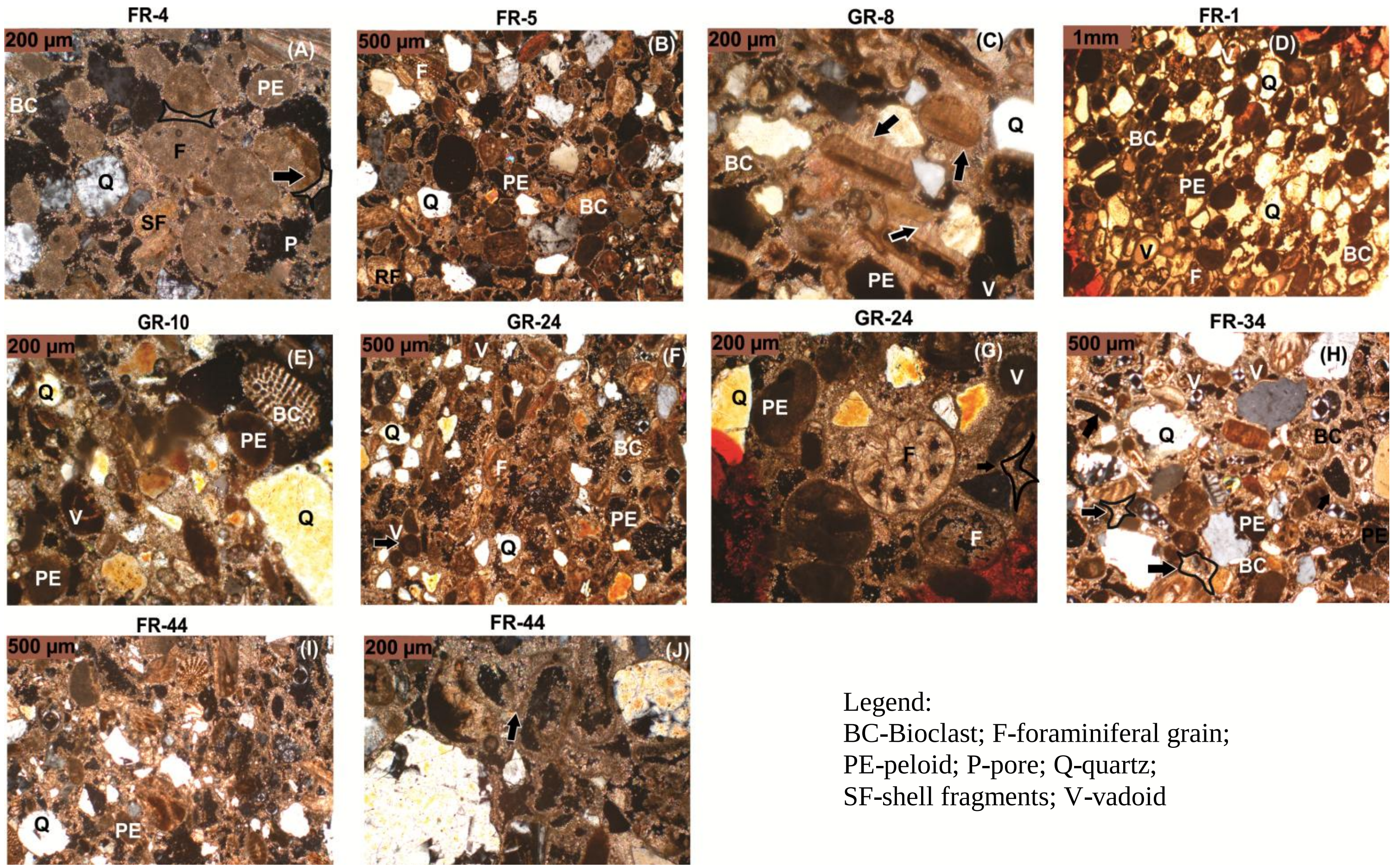

Legend:
BC-Bioclast; F-foraminiferal grain;
PE-peloid; P-pore; Q-quartz;
SF-shell fragments; V-vadoid

A- pellbiosparite, black arrow-miniscus fashion mostly originated in vadose environment-concave calcite cement to round off the pore space;

B-typical biopellsparite;
C-pellbiosparite, black arrow-fibrous needle columnar divulge cementation type and showing orientation of elongated allochems;

D-E-F- typical pellbiosparite;

G-pellbiosparite, 1st & 2nd order cement generation;

H-well-rounded clast of foraminifera bearing the signature of long distance transportation and reworking, elastic banding;

I-J-pellbiosparite, gravitational cement.

Fig 5.4 Thin section- photomicrographs of Miliolite, KHR, Kachchh.

Finer grains are better sorted and show a sharp difference in grain size with that of the coarser laminae (Fig. 5.4, B and D). Glennie (1970) has considered this feature to be one of the most important criteria for the identification of wind-deposited sand. It is also interesting to note that the elongated grains in obstacle deposits (mainly slip-face type) are arranged / oriented almost parallel to each other and to the laminae (Fig. 5.4, A, B, C and D.) The above phenomena have not been observed in fluvial reworked sheet miliolites (Fig. 5.4, E, G, H and J). This is obviously due to the selective deposition based on shapes of these grains along the slope of the obstacles provided by hills.

Sr. No	Field Location	Sample No.	Detritals %	Allochemical %		Cement nature calcareous micro sparite	Cement type	Mode of Occurrences Types	Residue %	Carbonates %
				Bioclast %	Peloid %					
1	O10	FR1	45	15	40	-do-	meniscus, gravitational	Type-I	36.95	63.05
2		FR2	50	25	25	-do-	meniscus	Type-I	42.85	57.15
3		FR3	80	10	10	-do-	meniscus	Type-I		
4	O9	FR4	35	30	35	-do-	meniscus	Type-I	45.00	55.00
5		FR5	45	25	30	-do-	blocky & granular.	Type-I	40.60	59.40
6	O5-O6	GR8	50	20	30	Fibrous rim niddle cement of magnesium calcite between bioclasts and non-carbonate lithoclasts in XPL. Fibrous cement between the bioclasts and non-carbonate lithoclasts in PPL		Type-I	42.15	57.85
7	F3	GR24	45	25	30	calcareous micro sparite	meniscus, gravitational	Type-I	36.60	63.40
8	O7	FR27						Type-I	37.60	62.40
9	F10	FR43						Type-I	38.90	61.10
10		FR44	55	20	25	-do-	meniscus	Type-I	48.00	52.00
11	O1	GR48	50	30	20	-do-	meniscus, gravitational	Type-I	44.50	55.50
		GR-49					meniscus, gravitational	Type-I	39.00	61.00
12	O8	FR57	45	25	30	-do-	meniscus, gravitational	Type-I	39.15	60.85
13	O12	KR62	55	25	20	-do-	meniscus	Type-I	49.60	50.40
14	O13	KR63	45	25	30	-do-	dog tooth spar	Type-I	34.90	65.10
15	O15	KR65	50	20	30	-do-	meniscus, gravitational	Type-I	42.80	57.20
16	F16	KR66	45	20	35	calcareous-micritic	granular to meniscus	Type-I	38.60	61.40
17	O16	VR69	45	20	35			Type-I	41.90	58.10
						Average Type-I Residue 41% and carbonates 59%			**699/17=41.12%**	**1000.9/17=58.88 %**
18	F3	GR25	60	15	25	-do-	granular to meniscus	Type-II	51.40	48.60
19	O2	GR50						Type-II	60.30	39.70
20	O3	GR52						Type-II	50.80	49.20
21	V3	GR54(A)						Type-II	61.70	38.30
22	O12	KR61	60	20	20	-do	meniscus	Type-II	58.40	41.60
23	O16	VR 68						Type-II	50.60	49.40
						Average Type-II Residue 55% and carbonates 45%			**333/6=55.50%**	**268.8/6=44.80 %**
24	F7	GR10	65	15	20	-do-	meniscus, gravitational	Type-III	59.90	40.10
25		GR11	70	10	20	-do-	gravitational	Type-III	66.85	33.15
26	F8	FR34	60	25	15	calcareous-micritic	meniscus	Type-III	64.15	35.50
27		FR37	60	20	20	-do-	meniscus	Type-III	53.15	46.85
28	F11	FR 45						Type-III	66.45	33.55
29	F12	FR-46						Type-III	68.00	32.00
30	O4	GR53						Type-III	73.60	26.40
31	V3	GR56						Type-III	81.40	18.60
32	V1	GR56(A)						Type-III	75.30	24.70
Over all Relative Detrital Allochems and Peloids Average			**1115/21= 53%**	**440/21= 21%**	**545/21= 26%**	**Average Type-III Residue 68% and carbonates 33%**			**609.15/09=67.68%**	**299.85/9=32.77%**
						Over all Relative Residues Average 51% and Carbonates 49%			**1641.45/32 =51.29%**	**1558.55/32 =48.70%**

Table 5.4 Relative frequency of detritals, allochems, cement and residues.

Scanning Electron Microscope (SEM) and
Energy Dispersive X-ray Spectroscopy (EDS) studies

A Scanning Electron Microscope (SEM) is Hitachi, Germany made electron microscope that produces images of a sample by scanning it with a focus beam electrons (Fig. 5.5a). The electrons interact with atoms in the sample, decoding samples surface topography and composition. Energy Dispersive X-ray Spectroscopy (EDS) can be done in conjunction with SEM by adding an X-ray detector analyzes X-ray by photons by energy, rather than wavelength, and can be used to chemically map a surface. The Energy Dispersive X-ray Spectroscopy (EDS) from Oxford Instruments; United Kingdom is a fully quantitative Silicon Drift Detectors (SDD) with excellent performance at low and high count rates and is suitable for applications that do not demand the full performance of the large area X-Max N detectors (Fig. 5.5b). Its detects elements from Be to Pu, Premium resolution of 125 eV available, guaranteed on your SEM, resolution measured in compliance with ISO 15632:2012,compatible with INCA® and AZtec® EDS analysis software.

Fig.5.5 a. Scanning Electron Microscope (SEM) Hitachi, Germany.

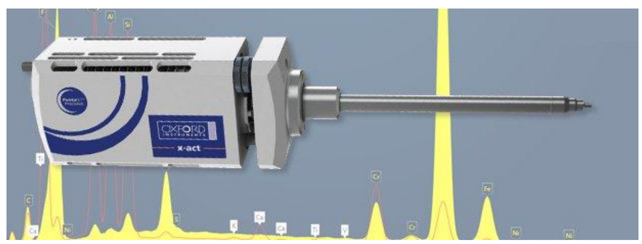

Fig.5.5 b. Energy Dispersive X-ray Spectroscopy (EDX),Oxford Instruments, UK.

It is reported for the first time in the present study that Type-I Miliolite of Gangeswar area (GR-8) exhibits presence of fibrous calcite as cement grown on the substrate of the peloid grain along with a very fine micrite layer (Fig. 5.6). This form of the pure calcite as indicated by the EDS study has been reported as mineral Lublinite by Stoops (1976) that has formed in limestone cave environment. The presence of Lublinite as cement therefore suggests a freshwater (continental) environment for the digenesis of the Type-I Miliolites.

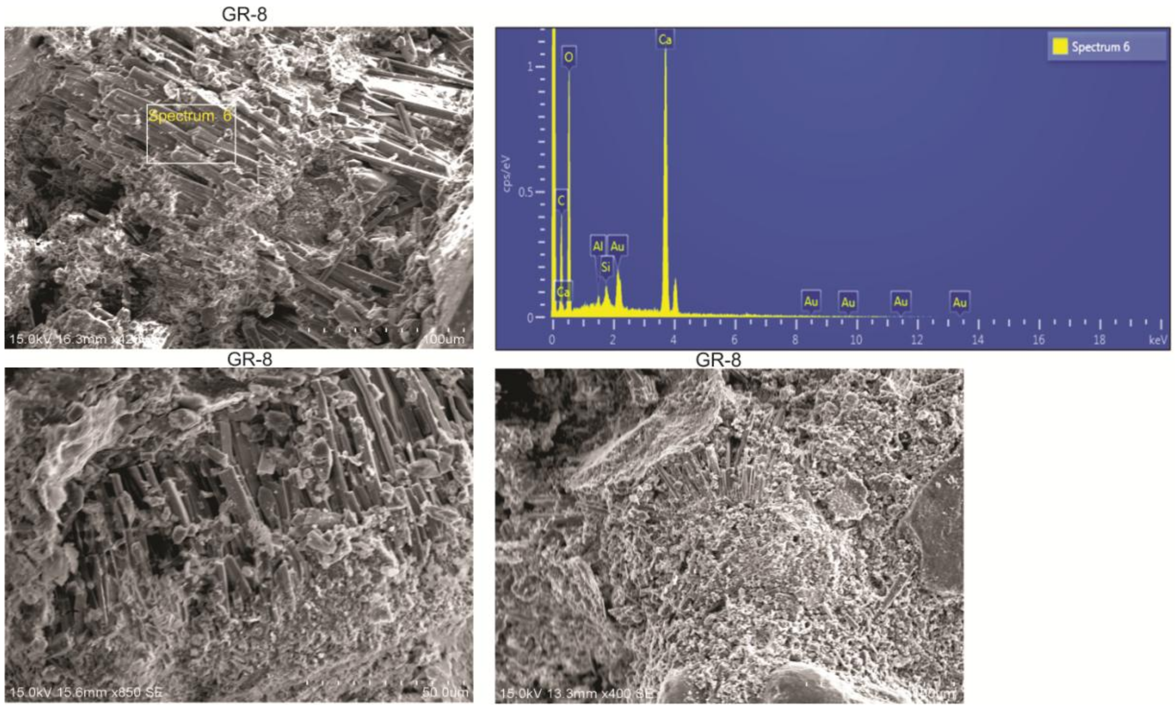

Fig.5.6 Fibrous form of calcite seen as cement in Type-I Miliolite from Gangeswar area. It is described as mineral 'Lublinite' by Stoops (1976).

The Type-II Miliolite samples are showing an overall granular nature of the micrite cement. At places rhombohedral form of the calcite cement could also be seen (Fig. 5.7). This indicate low magnesian nature of the calcite which is gain typically precipitating in the fresh water conditions. Looking to the nature and size of the cement grains it appears that the cemente precipitation must have occurred in vadose condition wherein the calcium carbonate saturated water doesn't remain for a longer time (Bhatt and Patel, 1998).

Type-III sample under SEM has indicated the presence of clay minerals (Fig. 5.8). This could be obviously due to the reworked nature of the sediments by local seasonal fluvial agencies that could mix the clays from the weathered substrate rocks. The EDS spectra indicate that these clays are complex hydrous alumina silicates of Na, K, Fe and Mg.

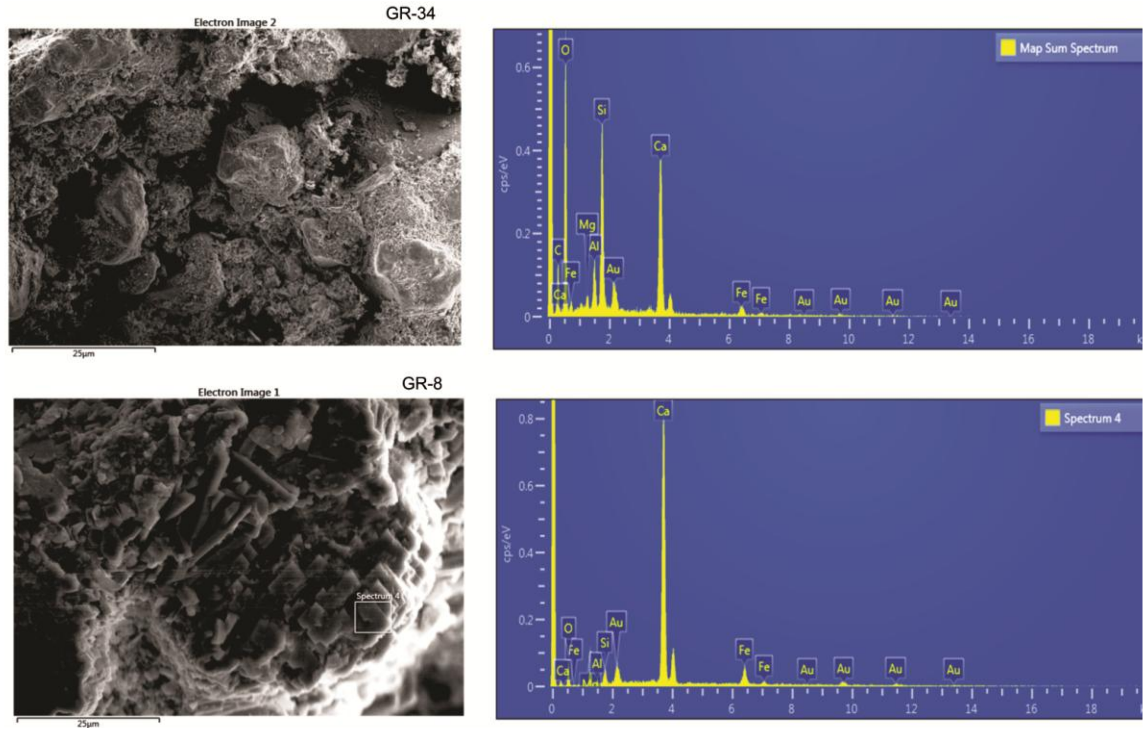

Fig. 5.7 Granular nature of the micritic grains and rhomboidal shape of the calcite cement in Type-II Miliolites. Presence of minor amount of Mg, Al and Fe peaks in EDS spectra indicate detrital impurities added to the pure calcareous nature of the Type-I deposits.

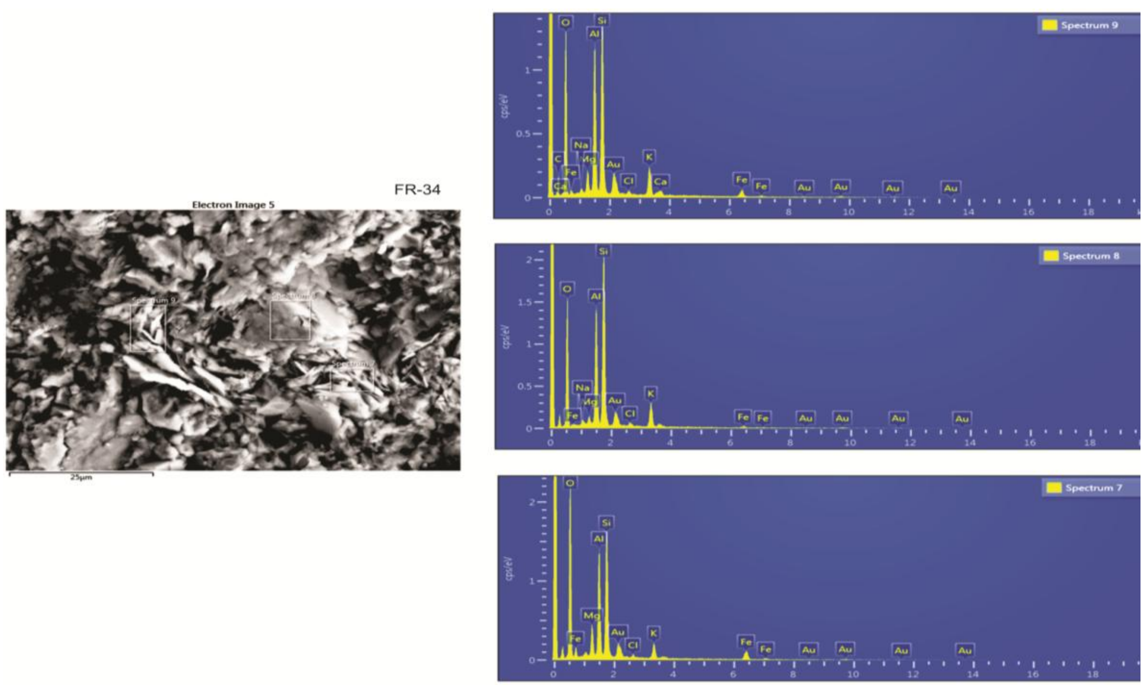

Fig. 5.8 Presence clay flaks of minerals in inter granular space in Type-III Miliolites. As EDS spectra show peaks of Mg, Fe, Na, K, and Al these could be the hydrous silicates representing the Illite-Kaolinite group of clays.

Geochemical Analysis (XRF)

The SPECTRO XEPOS HE (Fig. 5.9), Germany made is an advanced XRF spectrometer instrument for demanding applications, particularly for the analysis of environmental and process-critical elements and provides information about the elemental composition, empirical formula of pure material, surface contamination, and chemical / electronic state of elements.
X-ray fluorescence (XRF) spectrometry is a common tool for highly accurate and reproducible non-destructive element analyses. It is used routinely for investigation of a wide variety of materials such as minerals, rocks, slags, ceramics, metals, alloys, food, pharmaceuticals and fuels.

Fig. 5.9 X-Ray Fluorescence Spectroscopy (XRF) machine Spectro Xepos He.

Total 16 samples were grinded and made a homogeneous powder form. The sample tray with 12 positions for samples with diameters of 32/ 40/52 mm were run in ambient environment condition and analyzed in vacuumed condition. The SPECTRO XEPOS HE result analyzed with pre-installed hardware and software application packages analytical methods at the Institute of Seismological Research (ISR), Gandhinagar. Table 5.5 presents the selected oxides such as CaO, SiO_2, Al_2O_3 and K_2O for its abundance in all three types of the deposits and are further discussed in Chapter-7 for its significance. Table 5.6 enlist all elements which are mostly seen in microgram concentrations.

Sample No	Types	XRF Bond Values % out of total 57 bond elements			
		CaO %	**SiO_2 %**	**Al_2O3 %**	**K_2O %**
FR1	(Type-I)	45.86	16.96	7.727	0.4892
FR4	(Type-I)	50.72	11.13	5.109	0.3403
GR8	(Type-I)	49.79	11.46	4.305	0.3039
FR57	(Type-I)	45.06	16.5	5.174	0.4
KR62	(Type-I)	50.04	10.87	3.896	0.3335
KR63	(Type-I)	50	11.61	4.882	0.2836
VR69	(Type-I)	52.05	9.584	4.243	0.2377
	(Type-I)	**45% > and more**	**10 to 17 %**	**4 to 8 %**	**0.24 to 0.5%**
GR25	(Type-II)	43.92	18.39	6.537	0.4815
GR50	(Type-II)	34.51	26.19	11.2	0.9338
GR52	(Type-II)	9.003	48.06	22.73	1.532
GR54(A)	(Type-II)	23.14	39.24	14.89	1.118
	(Type-II)	**<44% and less**	**18 to 48%**	**6 to 23%**	**0.4to 1.5%**
GR10	(Type-III)	33.25	27.74	9.26	0.8157
FR34	(Type-III)	48.55	13.48	5.389	0.3197
FR45	(Type-III)	23.64	35.9	14.54	1.082
GR56	(Type-III)	11.48	44.55	17.7	1.403
GR56(A)	(Type-III)	29.82	32.83	12.96	1.034
	(Type-III)	**<34% and less except FR34**	**27 to 45%**	**5-18%**	**0.3 to1.4%**

Table 5.5 Geochemical Result of four bond elements XRF

Symbol	FR01 Concentration		FR04 Concentration		FR34 Concentration		FR45 Concentration		FR57 Concentration		GR08 Concentration		GR10 Concentration		GR25 Concentration	
Al_2O_3	7.727	%	5.109	%	5.389	%	14.54	%	5.174	%	4.305	%	9.26	%	6.537	%
SiO_2	16.96	%	11.13	%	13.48	%	35.9	%	16.5	%	11.46	%	27.74	%	18.39	%
P_2O_5	0.4366	%	0.4478	%	0.4366	%	0.2971	%	0.434	%	0.4731	%	0.3587	%	0.3462	%
S	907.9	µg/g	621.1	µg/g	660.7	µg/g	704.7	µg/g	714	µg/g	577.9	µg/g	547.5	µg/g	913.1	µg/g
Cl	208.7	µg/g	153.2	µg/g	374.7	µg/g	465.2	µg/g	142.1	µg/g	137.6	µg/g	173.4	µg/g	197.2	µg/g
K_2O	0.4892	%	0.3403	%	0.3197	%	1.082	%	0.4	%	0.3039	%	0.8157	%	0.4815	%
CaO	45.86	%	50.72	%	48.55	%	23.64	%	45.06	%	49.79	%	33.25	%	43.92	%
Sc	< 0.00029	%	< 0.0010	%	< 0.0010	%	< 0.0010	%	< 0.0010	%	< 0.0010	%	< 0.0010	%	< 0.0010	%
TiO_2	0.2981	%	0.2399	%	0.266	%	0.7912	%	0.2879	%	0.2001	%	0.4941	%	0.3438	%
V_2O_5	129.7	µg/g	102.5	µg/g	101.7	µg/g	206.6	µg/g	104.4	µg/g	97	µg/g	160.9	µg/g	125.7	µg/g
Cr_2O_3	85.5	µg/g	77.8	µg/g	67.7	µg/g	160.3	µg/g	79.9	µg/g	61.7	µg/g	108.6	µg/g	81.9	µg/g
MnO	586.8	µg/g	352.2	µg/g	1059	µg/g	690	µg/g	417.9	µg/g	361.2	µg/g	638.7	µg/g	436.5	µg/g
Fe_2O_3	3.11	%	2.479	%	2.76	%	6.649	%	3.71	%	2.65	%	3.903	%	3.184	%
CoO	< 11	µg/g	< 4.4	µg/g	< 3.8	µg/g	< 3.8	µg/g	< 4.5	µg/g	< 3.8	µg/g	< 3.8	µg/g	< 3.8	µg/g
NiO	20	µg/g	3.7	µg/g	10.7	µg/g	47.5	µg/g	19	µg/g	< 4.4	µg/g	24.8	µg/g	11.5	µg/g
CuO	24.5	µg/g	9.5	µg/g	22.3	µg/g	28.8	µg/g	45.2	µg/g	30.8	µg/g	28	µg/g	34.1	µg/g
ZnO	36.5	µg/g	29	µg/g	29.4	µg/g	77.1	µg/g	38.6	µg/g	26.8	µg/g	53.5	µg/g	38	µg/g
Ga	9.7	µg/g	8.3	µg/g	7.2	µg/g	16.9	µg/g	9.1	µg/g	7.4	µg/g	11.9	µg/g	8.3	µg/g
Ge	< 0.5	µg/g	< 0.5	µg/g	< 0.5	µg/g	< 0.5	µg/g	< 0.5	µg/g	< 0.5	µg/g	< 0.5	µg/g	< 0.5	µg/g
As_2O_3	27.8	µg/g	20.6	µg/g	13.5	µg/g	12.8	µg/g	7.1	µg/g	15.9	µg/g	11.7	µg/g	6.4	µg/g
Se	0.5	µg/g	0.7	µg/g	< 0.5	µg/g	< 0.5	µg/g	< 0.3	µg/g	< 0.1	µg/g	< 0.5	µg/g	< 0.3	µg/g
Br	7	µg/g	1.6	µg/g	0.6	µg/g	7.1	µg/g	1.9	µg/g	1.4	µg/g	1.4	µg/g	1.9	µg/g
Rb_2O	25.1	µg/g	20.2	µg/g	18.1	µg/g	57.2	µg/g	22.2	µg/g	17.1	µg/g	45.8	µg/g	28.1	µg/g
SrO	1093	µg/g	1269	µg/g	626.3	µg/g	552.3	µg/g	897.7	µg/g	1186	µg/g	1253	µg/g	1186	µg/g
Y	7.1	µg/g	8.2	µg/g	9.9	µg/g	29.1	µg/g	9.5	µg/g	6.4	µg/g	16.7	µg/g	9.5	µg/g
ZrO_2	89.3	µg/g	217.5	µg/g	186.3	µg/g	648.5	µg/g	232.9	µg/g	153.4	µg/g	358.8	µg/g	209.9	µg/g
Nb_2O_5	5.2	µg/g	5.3	µg/g	6.3	µg/g	16.4	µg/g	8.2	µg/g	4.9	µg/g	13.3	µg/g	5.7	µg/g
MoO	< 0.6	µg/g	0.4	µg/g	< 0.6	µg/g	< 0.6	µg/g	< 1.0	µg/g	< 0.6	µg/g	< 0.6	µg/g	< 0.9	µg/g
Ru	< 0.5	µg/g	< 0.5	µg/g	< 0.5	µg/g	< 0.5	µg/g	< 0.5	µg/g	< 0.5	µg/g	< 0.5	µg/g	< 0.5	µg/g
Rh	< 0.5	µg/g	< 0.5	µg/g	< 0.5	µg/g	< 0.5	µg/g	< 0.5	µg/g	< 0.5	µg/g	< 0.5	µg/g	< 0.5	µg/g
Pd	< 0.5	µg/g	< 0.5	µg/g	< 0.5	µg/g	< 0.5	µg/g	< 0.5	µg/g	< 0.5	µg/g	< 0.5	µg/g	< 0.5	µg/g
Ag	< 0.5	µg/g	< 0.5	µg/g	< 0.5	µg/g	< 0.5	µg/g	< 0.5	µg/g	< 0.5	µg/g	< 0.5	µg/g	< 0.5	µg/g
Cd	< 0.3	µg/g	0.8	µg/g	< 0.4	µg/g	< 0.3	µg/g	< 0.4	µg/g	< 0.3	µg/g	< 0.1	µg/g	< 0.1	µg/g
In	3.9	µg/g	2.8	µg/g	4.2	µg/g	3.1	µg/g	4.1	µg/g	3.8	µg/g	4.6	µg/g	2.3	µg/g
SnO_2	1.9	µg/g	< 0.6	µg/g	4.4	µg/g	1.2	µg/g	12.2	µg/g	2.6	µg/g	2.4	µg/g	4.7	µg/g
Sb_2O_5	< 0.7	µg/g	< 0.7	µg/g	< 0.7	µg/g	< 0.7	µg/g	< 0.7	µg/g	< 0.7	µg/g	< 0.7	µg/g	< 0.7	µg/g
Te	< 0.5	µg/g	< 0.5	µg/g	< 0.5	µg/g	< 0.5	µg/g	< 0.5	µg/g	< 0.5	µg/g	< 0.5	µg/g	< 0.5	µg/g
I	< 0.7	µg/g	< 0.7	µg/g	< 0.7	µg/g	3.9	µg/g	< 0.7	µg/g	< 0.7	µg/g	< 0.7	µg/g	< 0.7	µg/g
Cs	6.1	µg/g	7.6	µg/g	4	µg/g	6.6	µg/g	5.2	µg/g	5.5	µg/g	8.7	µg/g	4.2	µg/g
BaO	130	µg/g	188.9	µg/g	166.6	µg/g	270.9	µg/g	437.6	µg/g	288.8	µg/g	240.3	µg/g	146.4	µg/g
La_2O_3	51.2	µg/g	46.1	µg/g	38.8	µg/g	63	µg/g	40	µg/g	44.2	µg/g	59.7	µg/g	41.9	µg/g
Ce_2O_3	< 3.0	µg/g	< 3.0	µg/g	< 3.0	µg/g	19.5	µg/g	< 3.0	µg/g	< 3.0	µg/g	7.9	µg/g	< 3.0	µg/g
Pr	< 4.0	µg/g	< 4.0	µg/g	< 4.0	µg/g	< 4.0	µg/g	< 4.0	µg/g	< 4.0	µg/g	< 4.0	µg/g	< 4.0	µg/g
Nd	27.8	µg/g	< 5.1	µg/g	< 12	µg/g	< 9.8	µg/g	19.2	µg/g	25.8	µg/g	12.1	µg/g	< 11	µg/g
Sm	66.6	µg/g	70.5	µg/g	79.6	µg/g	56.9	µg/g	62.1	µg/g	71.3	µg/g	55.2	µg/g	61.2	µg/g
Hf	< 2.0	µg/g	< 2.0	µg/g	< 2.0	µg/g	< 2.0	µg/g	< 2.0	µg/g	< 2.0	µg/g	< 2.0	µg/g	< 2.0	µg/g
Ta_2O_5	< 2.0	µg/g	< 2.0	µg/g	< 2.0	µg/g	< 2.0	µg/g	< 2.0	µg/g	< 2.0	µg/g	< 2.0	µg/g	< 2.0	µg/g
WO_3	< 1.5	µg/g	< 1.5	µg/g	< 1.5	µg/g	< 1.5	µg/g	< 1.5	µg/g	< 1.5	µg/g	< 1.5	µg/g	< 2.8	µg/g
Au	< 1.1	µg/g	< 1.1	µg/g	< 1.0	µg/g	< 1.0	µg/g	< 1.1	µg/g	< 1.1	µg/g	< 1.0	µg/g	< 1.1	µg/g
Hg	< 0.7	µg/g	< 1.0	µg/g	< 0.7	µg/g	< 0.7	µg/g	1.4	µg/g	< 0.7	µg/g	< 0.7	µg/g	< 0.9	µg/g
Tl	< 0.7	µg/g	2.3	µg/g	< 0.7	µg/g	< 0.7	µg/g	1.4	µg/g	< 0.7	µg/g	< 0.7	µg/g	1.3	µg/g
Pb	18	µg/g	14.9	µg/g	14.4	µg/g	22.3	µg/g	16.9	µg/g	14.3	µg/g	22.7	µg/g	14.4	µg/g
Bi	< 0.5	µg/g	< 0.5	µg/g	< 0.5	µg/g	< 0.5	µg/g	< 0.5	µg/g	< 0.5	µg/g	< 0.5	µg/g	< 0.5	µg/g
Th	8	µg/g	10.3	µg/g	6.9	µg/g	18.4	µg/g	8.2	µg/g	6.2	µg/g	11.2	µg/g	8.3	µg/g
U	4.9	µg/g	7	µg/g	0.9	µg/g	4.2	µg/g	3.6	µg/g	6.2	µg/g	7.8	µg/g	5.6	µg/g

Table 5.6 (1) Geochemical Results of bond elements of Miliolite, KHF, Kachchh.

	GR50		GR52		GR54A		GR56		GR56A		KR61		KR63		KR69	
Symbol	Concentration		Concentration		Concentration		Concentration		Concentration		Concentration		Concentration		Concentration	
Al2O3	11.2	%	22.73	%	14.89	%	17.7	%	12.96	%	3.896	%	4.882	%	4.243	%
SiO2	26.19	%	48.06	%	39.24	%	44.55	%	32.83	%	10.87	%	11.61	%	9.584	%
P2O5	0.557	%	0.1282	%	0.3427	%	0.3004	%	0.3758	%	0.4381	%	0.4205	%	0.5403	%
S	1108	µg/g	730.8	µg/g	736.4	µg/g	677	µg/g	791.7	µg/g	591.4	µg/g	751.5	µg/g	492.2	µg/g
Cl	616.9	µg/g	262.9	µg/g	213.2	µg/g	197.9	µg/g	132.6	µg/g	293.5	µg/g	266.9	µg/g	162.9	µg/g
K2O	0.9338	%	1.532	%	1.118	%	1.403	%	1.034	%	0.3335	%	0.2836	%	0.2377	%
CaO	34.51	%	9.003	%	23.14	%	11.48	%	29.82	%	50.04	%	50	%	52.05	%
Sc	< 0.0062	%	0.0021	%	< 0.0010	%	< 0.0015	%	< 0.0010	%	< 0.0010	%	< 0.0010	%	< 0.0010	%
TiO2	0.5974	%	1.369	%	0.7452	%	0.9633	%	0.7001	%	0.2394	%	0.2597	%	0.1583	%
V2O5	197.6	µg/g	339	µg/g	256.2	µg/g	318.5	µg/g	229.9	µg/g	100.1	µg/g	120.9	µg/g	97.1	µg/g
Cr2O3	131.7	µg/g	230.5	µg/g	158.4	µg/g	193.4	µg/g	144.9	µg/g	92.6	µg/g	78.1	µg/g	50.5	µg/g
MnO	488	µg/g	324.2	µg/g	511.1	µg/g	752.2	µg/g	666.9	µg/g	417.3	µg/g	514.8	µg/g	400.9	µg/g
Fe2O3	4.502	%	7.328	%	7.762	%	12.07	%	5.322	%	2.526	%	2.51	%	2.018	%
CoO	< 0.5	µg/g	< 6.8	µg/g	27.2	µg/g	13.8	µg/g	< 3.8	µg/g	< 3.8	µg/g	< 3.8	µg/g	< 8.9	µg/g
NiO	29.2	µg/g	41.1	µg/g	54.1	µg/g	60.2	µg/g	34.7	µg/g	10.6	µg/g	10.8	µg/g	< 4.7	µg/g
CuO	28.1	µg/g	41.3	µg/g	36.4	µg/g	41.1	µg/g	34.3	µg/g	33.6	µg/g	23.2	µg/g	56.3	µg/g
ZnO	46.5	µg/g	72.4	µg/g	81.7	µg/g	127.8	µg/g	63	µg/g	80.5	µg/g	26.6	µg/g	23.3	µg/g
Ga	13.4	µg/g	28.8	µg/g	17.6	µg/g	21.6	µg/g	14.1	µg/g	6.5	µg/g	8.1	µg/g	5.2	µg/g
Ge	< 0.5	µg/g	0.8	µg/g	< 0.5	µg/g	< 0.5	µg/g	< 0.5	µg/g	< 0.5	µg/g	< 0.5	µg/g	< 0.5	µg/g
As2O3	16.1	µg/g	14.7	µg/g	17.9	µg/g	18.8	µg/g	15.9	µg/g	11	µg/g	6	µg/g	12.6	µg/g
Se	< 0.1	µg/g	< 0.1	µg/g	< 0.5	µg/g	< 0.5	µg/g	< 0.5	µg/g	1	µg/g	< 0.1	µg/g	0.4	µg/g
Br	70.4	µg/g	19.6	µg/g	22.3	µg/g	8.2	µg/g	15.9	µg/g	3.3	µg/g	3.3	µg/g	2.8	µg/g
Rb2O	46.5	µg/g	104.9	µg/g	62	µg/g	79	µg/g	51	µg/g	19.8	µg/g	14.6	µg/g	13.6	µg/g
SrO	413.7	µg/g	328.7	µg/g	728.5	µg/g	486.9	µg/g	526.9	µg/g	2237	µg/g	1078	µg/g	1448	µg/g
Y	19.1	µg/g	21	µg/g	21.7	µg/g	30.7	µg/g	18.1	µg/g	4.7	µg/g	4.5	µg/g	3.7	µg/g
ZrO2	408.5	µg/g	436.1	µg/g	340.3	µg/g	477.3	µg/g	458.3	µg/g	120.8	µg/g	86.4	µg/g	55.7	µg/g
Nb2O5	13.3	µg/g	24.6	µg/g	18.1	µg/g	21.1	µg/g	14.8	µg/g	3.5	µg/g	4.2	µg/g	1.3	µg/g
MoO	< 0.6	µg/g	< 0.6	µg/g	< 0.6	µg/g	1.2	µg/g	< 1.0	µg/g	< 0.9	µg/g	< 0.8	µg/g	< 0.6	µg/g
Ru	< 0.5	µg/g	< 0.5	µg/g	< 0.5	µg/g	< 0.5	µg/g	< 0.5	µg/g	< 0.5	µg/g	< 0.5	µg/g	< 0.5	µg/g
Rh	< 0.5	µg/g	< 0.5	µg/g	< 0.5	µg/g	< 0.5	µg/g	< 0.5	µg/g	< 0.5	µg/g	< 0.5	µg/g	< 0.5	µg/g
Pd	< 0.5	µg/g	< 0.5	µg/g	< 0.5	µg/g	< 0.5	µg/g	< 0.5	µg/g	< 0.5	µg/g	< 0.5	µg/g	< 0.5	µg/g
Ag	< 0.5	µg/g	< 0.5	µg/g	< 0.5	µg/g	0.4	µg/g	< 0.5	µg/g	< 0.5	µg/g	< 0.5	µg/g	< 0.5	µg/g
Cd	< 0.3	µg/g	< 0.1	µg/g	< 0.1	µg/g	< 0.1	µg/g	< 0.1	µg/g	< 0.2	µg/g	< 0.2	µg/g	< 0.3	µg/g
In	3.4	µg/g	2.1	µg/g	5	µg/g	1.8	µg/g	3.5	µg/g	3.2	µg/g	3	µg/g	3.3	µg/g
SnO2	0.5	µg/g	2.4	µg/g	6.1	µg/g	1.3	µg/g	1	µg/g	< 0.6	µg/g	< 0.6	µg/g	13.4	µg/g
Sb2O5	< 0.7	µg/g	< 0.7	µg/g	< 0.7	µg/g	< 0.7	µg/g	< 0.7	µg/g	< 0.7	µg/g	< 0.7	µg/g	< 0.7	µg/g
Te	< 0.5	µg/g	< 0.5	µg/g	< 0.5	µg/g	< 0.5	µg/g	< 0.5	µg/g	< 0.5	µg/g	< 0.5	µg/g	< 0.5	µg/g
I	30.3	µg/g	9.5	µg/g	6.2	µg/g	0.8	µg/g	3.2	µg/g	< 0.7	µg/g	0.8	µg/g	< 0.7	µg/g
Cs	9	µg/g	7.2	µg/g	7.7	µg/g	7.2	µg/g	5.9	µg/g	< 1.0	µg/g	< 1.0	µg/g	6	µg/g
BaO	276.9	µg/g	202.2	µg/g	230.1	µg/g	329.6	µg/g	248	µg/g	179.5	µg/g	86.9	µg/g	96.2	µg/g
La2O3	58.7	µg/g	53.3	µg/g	54	µg/g	56.3	µg/g	50.8	µg/g	36.6	µg/g	34.8	µg/g	39.5	µg/g
Ce2O3	< 6.7	µg/g	19.8	µg/g	< 3.0	µg/g	26.7	µg/g	< 3.0	µg/g	< 3.0	µg/g	< 3.0	µg/g	< 3.0	µg/g
Pr	< 4.0	µg/g	< 4.0	µg/g	< 4.0	µg/g	< 4.0	µg/g	< 4.0	µg/g	< 4.0	µg/g	< 4.0	µg/g	< 4.0	µg/g
Nd	14.6	µg/g	< 5.1	µg/g	< 10	µg/g	10.1	µg/g	< 5.1	µg/g	< 11	µg/g	< 5.1	µg/g	10.6	µg/g
Sm	56.7	µg/g	25.7	µg/g	54.8	µg/g	54.6	µg/g	61.2	µg/g	73.1	µg/g	75.7	µg/g	84.1	µg/g
Hf	< 2.0	µg/g	< 2.0	µg/g	< 2.0	µg/g	< 3.5	µg/g	< 2.0	µg/g	< 2.0	µg/g	< 2.0	µg/g	< 2.0	µg/g
Ta2O5	< 2.0	µg/g	< 2.0	µg/g	< 2.0	µg/g	< 2.0	µg/g	< 2.0	µg/g	< 2.0	µg/g	< 2.0	µg/g	< 2.0	µg/g
WO3	< 1.5	µg/g	1.8	µg/g	< 1.5	µg/g	< 1.5	µg/g	< 1.5	µg/g	< 1.5	µg/g	< 2.9	µg/g	< 1.5	µg/g
Au	< 1.0	µg/g	< 0.9	µg/g	< 1.0	µg/g	< 1.1	µg/g	< 1.0	µg/g	< 1.2	µg/g	< 1.1	µg/g	< 1.1	µg/g
Hg	< 0.7	µg/g	< 0.7	µg/g	< 0.7	µg/g	< 0.6	µg/g	< 0.7	µg/g	< 0.7	µg/g	< 0.7	µg/g	1.6	µg/g
Tl	< 0.7	µg/g	< 0.7	µg/g	< 0.7	µg/g	< 0.7	µg/g	< 0.7	µg/g	2.4	µg/g	< 0.8	µg/g	1.2	µg/g
Pb	18.9	µg/g	28.6	µg/g	24.2	µg/g	29.6	µg/g	20.4	µg/g	17.1	µg/g	12.5	µg/g	13.5	µg/g
Bi	< 0.5	µg/g	< 0.5	µg/g	< 0.5	µg/g	< 0.5	µg/g	< 0.5	µg/g	< 0.5	µg/g	< 0.5	µg/g	< 0.5	µg/g
Th	13.3	µg/g	21	µg/g	13.9	µg/g	20.5	µg/g	11.4	µg/g	7.3	µg/g	5.1	µg/g	5.5	µg/g
U	3.7	µg/g	5	µg/g	4.2	µg/g	6	µg/g	1.8	µg/g	11.8	µg/g	3.9	µg/g	6.4	µg/g

Table 5.6 (2) Geochemical Results of bond elements of Miliolite, KHF, Kachchh.

Magnetic Susceptibility (MS)

Bulk magnetic susceptibility measurements on sedimentological samples from all geological periods have been used widely in the last two decades for correlations and as a proxy for sea-level variations. Mineral magnetic approach can be favored tool for resolving climate conditions that prevailing during Quaternary. Magnetic measurement is easy and rapidly made in the laboratory with highly accurate apart from being non-destructive. The property of samples can be used to carry out sediment provenance and paleoclimate reconstruction (Basvaiah and Khadkikar, 2004). MS is the degree to which a material can be magnetized in an external magnetic field. If the ratio between the induced magnetization and the inducing field is expressed per unit volume, volume susceptibility (K) is determine as K=M/H, where M is the volume magnetization induced in a material susceptibility k by the applied external field H. Susceptibility is define as x=k / r, where r is the density of the material.

Total 27 samples from three distinct types of deposits and different parts of the study area were analysed for mass-normalized magnetic susceptibility which is volume magnetic susceptibility multiplied by a reference volume of 1 m^3 and divided by the sample mass expressed as Kmass (m^3/kg). Measurements are made on each sample weighed with a precision of 0.001 g. The used data presented represent an average of the three measurements. Magnetic susceptibility measurements were performed on multifunction Kappa bridge (MFK-1B) at Geology Department of the Maharaja Sayajirao University of Baroda. The Kappabridge KLY2 magnetic susceptibility system (Fig. 5.10) measures MS and AMS of hard rock or sediment samples at sensitivities of 0.05 x 10^{-6} SI to 200,000 x 10^{-6} SI within a series of 11 ranges. Precision is 2 x 10^{-6} (SI). This study compares the MS evolution with geomorphic settings parameters. MS measurements were made on the same samples used for thin section and residual analysis both. The sampling rate applied was different depending on the outcrop settings. Table 5.7 presents the results of this study.

Fig.5.10 Kappa bridge (MFK-1B) AGICO
(Advanced Geoscience Instruments Co. Czech, Republic).

FreqVa [Hz]	Field [A/m]	Volume [cm3]	HolderRe [SI]	HolderIm [SI]	Time	Date	Note
976	200	7.97	-5.756E-06	-289.0E-09	18:15:13	27-02-2017	Average of Range 3

Sr.No.	Sample Codes	Mass [g]	Kre [SI]	Kim [SI]	Kvol [SI]	Kmass [m3/kg]	Ph	Residue %	Type
1	FR-01	11.82	513.333E-06	5.617E-06	644.1E-06	434.3E-09	0.63	36.95	Type-I
2	FR-02	12.09	321.700E-06	3.504E-06	403.7E-06	266.2E-09	0.63	42.85	Type-I
3	GR-08	11.98	507.133E-06	3.270E-06	636.3E-06	423.3E-09	0.37	42.15	Type-I
4	GR-24	11.86	457.367E-06	4.513E-06	573.9E-06	385.5E-09	0.56	36.60	Type-I
5	FR-27	11.18	759.367E-06	8.939E-06	952.8E-06	679.3E-09	0.68	37.60	Type-I
6	FR-43	12.23	212.900E-06	2.072E-06	267.1E-06	174.0E-09	0.55	38.90	Type-I
7	GR-48	10.98	394.400E-06	2.943E-06	494.8E-06	359.3E-09	0.43	44.50	Type-I
8	GR-49	11.52	009.185E-06	2.837E-07	011.5E-06	008.0E-09	1.77	39.00	Type-I
9	FR-57	11.99	614.867E-06	4.899E-06	771.5E-06	512.9E-09	0.46	39.15	Type-I
10	KR-62	11.61	590.033E-06	7.468E-06	740.3E-06	508.3E-09	0.72	49.60	Type-I
11	KR-65	12.72	538.633E-06	5.971E-06	675.8E-06	423.4E-09	0.63	42.80	Type-I
12	KR-66	11.66	269.400E-06	4.518E-06	338.0E-06	231.0E-09	0.96	38.60	Type-I
13	VR-69	11.97	631.033E-06	6.101E-06	791.8E-06	527.3E-09	0.55	41.90	Type-I
14	GR-25	12.07	455.167E-06	3.152E-06	571.1E-06	377.1E-09	0.39	51.40	Type-II
15	GR50	11.84	360.667E-06	9.391E-06	452.5E-06	304.6E-09	1.49	60.30	Type-II
16	GR-52	11.09	171.167E-06	3.825E-06	214.8E-06	154.3E-09	1.28	50.80	Type-II
17	GR-54(A)	11.55	522.633E-06	1.291E-06	655.8E-06	452.3E-09	1.42	61.70	Type-II
18	GR-10	11.89	398.633E-06	2.585E-06	500.2E-06	335.2E-09	0.37	59.90	Type-III
19	GR-11	12.61	503.333E-06	2.507E-06	631.5E-06	399.1E-09	0.29	66.85	Type-III
20	FR-34	11.47	448.500E-06	6.704E-06	562.7E-06	390.9E-09	0.86	60.00	Type-III
21	FR-37	12.16	546.400E-06	3.343E-06	685.6E-06	449.2E-09	0.35	53.15	Type-III
22	FR-44	12.02	374.833E-06	2.488E-06	470.3E-06	311.8E-09	0.38	48.00	Type-III
23	FR-45	12.26	607.533E-06	9.202E-06	762.2E-06	495.5E-09	0.87	66.45	Type-III
24	FR-46	12.42	458.200E-06	3.133E-06	574.9E-06	368.9E-09	0.39	68.00	Type-III
25	GR-53	12.08	660.667E-06	4.273E-06	828.9E-06	546.7E-09	0.37	73.60	Type-III
26	GR-56	12.27	357.867E-06	4.730E-06	449.0E-06	291.7E-09	0.77	81.40	Type-III
27	GR-56(A)	11.84	476.100E-06	6.842E-06	597.4E-06	402.2E-09	0.82	75.30	Type-III

Table-5.7 Magnetic Susceptibility values of miliolite samples.

In this study the relationship between the average magnitudes of bulk MS in three classified occurrences types of Miliolite deposits was explored. The relationship between types and mean magnetic susceptibility can help us to understand the origin of MS variations. If the detrital grains were derived from the Deccan Trap basalt which occurs in the southern side of the KHR, (KR.62.65 and 66) perhaps an increased value of MS could have been seen. Overall well sorted and dominant calcareous nature of the Type-I and Type-II deposits could also be established by the fact that they have yielded quite low values of magnetic susceptibility.